International Journal of Infrared and Millimeter Waves, Vol. 18, No. 2, 1997

A WIDE-FIELD RELAY OPTICS SYSTEM FOR THE CALTECH SUBMILLIMETER OBSERVATORY

E. Serabyn

California Institute of Technology, 320-47
Pasadena, California 91125

Received November 4, 1996

ABSTRACT

Relay optics designed for use with imaging arrays at the Caltech Submillimeter Observatory are described. An off-axis ellipsoidal mirror with foci displaced from the conjugate planes is used to achieve a Strehl ratio > 0.88 over a $2'$ square field of view (corresponding to a far field of 15×15 diffraction beams) at a wavelength of 350 μm. The mirror also provides an aperture-stop image just prior to focus which allows compact entry into cryogenic camera dewars. Using a compensating ellipsoid in subsequent camera optics, the Strehl ratio can be improved to > 0.95 at all points across the field, even for off-axis chop angles of the telescope's secondary mirror as large as $2'$.

Keywords: optical design, relay optics, ellipsoidal mirrors

I. INTRODUCTION

The advent of submillimeter-wavelength imaging cameras [1-4] should enable advances in submillimeter astronomy as striking as those which have recently transformed infrared astronomy [5]. Indeed, shorter mapping times, greater data uniformity, and increased immunity to atmospheric fluctuations are more critical in the submillimeter case, where even at high mountain sites the atmospheric opacity's magnitude and temporal fluctuations both tend to be quite large. However, to make the most of these emerging capabilities, optimization is required not only of telescopes and detector arrays, but also of intervening relay optics. This paper discusses constraints on relay optics systems which are specific to operation at these long infrared wavelengths ($\lambda = 300$ μm to 1000 μm), and presents the design of the successful dual-instrument relay optics system in

0195-9271/97/0200-0273$12.50/0

use at the Caltech Submillimeter Observatory (CSO).

The basic goal of any relay optics system is to maintain high-quality imaging while transforming the beam focal ratio from that provided by the telescope to that required by detector arrays. In the case of the CSO, the chopping secondary mirror has a focal ratio, F_o = 12.36, which needs to be converted to an instrumental focal ratio, F_i, of about 4 to 5, so that in the shortest wavelength submillimeter atmospheric windows (450 μm and 350 μm), the focal-plane diffraction spot size, $F_i\lambda$, matches pixel sizes (1 – 2 mm) of available monolithic submillimeter detector arrays [6].

Extant submillimeter telescopes are typically classical Cassegrains with highly curved primary and secondary mirrors. These mirrors' short radii of curvature result in astigmatism and field curvature, respectively, which limit the unaberrated field-of-view (FOV) at the Cassegrain focus to a diameter on the order of a hundred diffraction beamwidths [7,8]. Such unaberrated fields are much larger than the sizes of monolithic submillimeter detector arrays foreseen for the immediate future, which at best can cover a diameter of 10 to 20 diffraction beams. Thus, available array sizes set the performance requirements on the relay optics. However, maintaining image quality over even such a seemingly relaxed FOV is nontrivial at long wavelengths, for several reasons. First, due to high absorption in candidate lens materials at submillimeter wavelengths [9], only all-reflective systems are viable. Second, large diffraction spot sizes at long wavelengths ($F_o\lambda \sim$ 4 to 12 mm for λ = 300 to 1000 μm at the CSO's Cassegrain focus) imply large off-axis displacements for relatively few diffraction beams (i.e., 10 diffraction beams at λ = 400 μm correspond to the same spatial scale as 2000 beams at λ = 2 μm). Third, long wavelengths also imply unacceptably high diffraction losses at small apertures, ruling out designs in use at shorter wavelengths which include small mirrors and/or apertures. Thus, solutions based on large and unobscured off-axis mirrors are mandated. In the case of the CSO, the secondary desire to provide two equivalent instrument foci in order to easily accomodate both "in house" and "visitor" instruments adds the goal of compactness, and finally, simplicity is required in order to allow for applicability to a wide range of future instruments.

II. ELLIPSOIDAL MIRRORS

The simplest reflective reimaging system consists of a single off-axis section of an ellipsoidal mirror, which reimages one of the ellipsoid's two geometric foci to its second. This approach has been the standard for single-pixel submillimeter detectors, where FOV is not an issue, but as the imaging performance at small focal ratios degrades quickly for increasing off-axis object distances, this approach is questionable for detector arrays. Nevertheless, as simplicity is paramount in a relay optics system intended for general use by multiple instruments, simple variations on the single ellipsoidal mirror scenario were explored

in order to determine if this most basic design could be made to perform adequately. Numerical evaluation of the designs considered was carried out with the aid of the Code V optical design software package [10].

The starting point for the analysis was a standard off-axis ellipsoidal design. An off-axis section of an ellipsoid of revolution was chosen to convert the CSO's input beam to a relayed $F_1 = 4.5$ focus, with the chief ray from the field center undergoing a reflection of 38°. Smaller reflection angles would yield smaller aberrations, but angles of this order allow redirection of the focused beam down

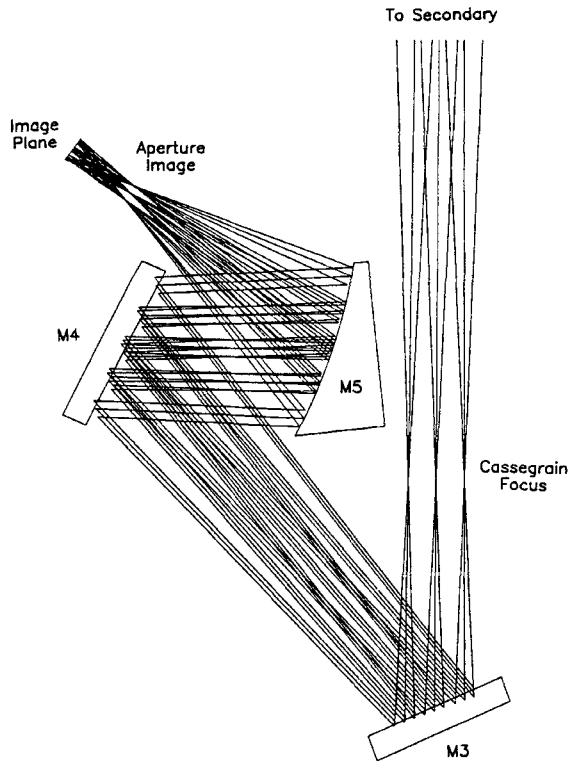

Figure 1: Relay optics schematic layout. The rays plotted are for a 2′ square FOV in the telescope's far-field. The light from the secondary mirror is first reflected at the flat (front-surface-aluminized glass) mirrors M3 and M4, and then at the (numerically-milled aluminum) off-axis ellipsoid M5. The size of M5 is 0.35 × 0.38 m, and the beam footprint on M5 has a diameter of 0.14 m. In the diagram, the plotted rays do not reflect exactly on M3 and M4 because these mirrors are tipped slightly out of the plane of the diagram to allow for two symmetric instrumental foci slightly in front of and behind the plane of the paper (with duplicate M4's and M5's). M3 is turntable-mounted to allow selection of the subsequent mirror pair. An image of the secondary, of diameter 32 mm, lies 142 mm before the relayed focal plane.

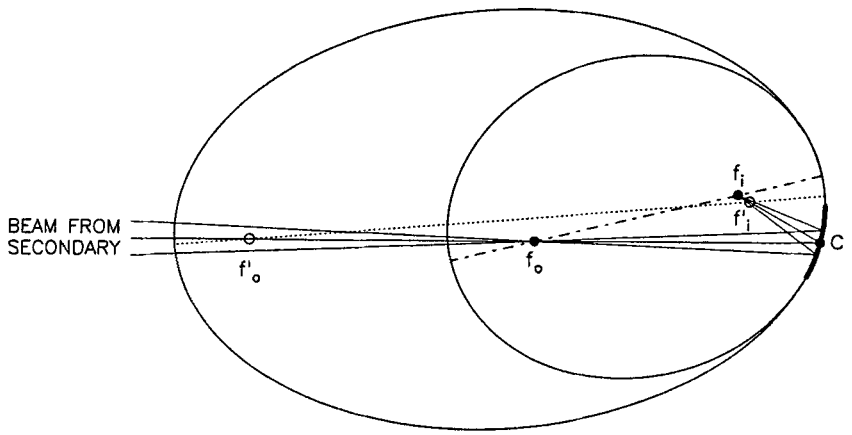

Figure 2: Cross-section of the ellipsoidal mirror geometry, in the plane containing the telescope and ellipsoid axes. Both the initial (smaller) and modified (larger) elliptical cross-sections are shown. The off-axis mirror section, with center at **C**, is shown in bold. The chief ray and two edge rays for the secondary's F/12.4 beam are also shown, as are the two ellipses' major axes (dash-dot and dotted lines). Both ellipses reimage the object plane normal to the chief ray at f_o = 1803 mm (the telescope's Cassegrain focal plane) to the image plane at f_i = 642 mm, but only the smaller ellipse has its foci (filled circles) at the intersections of the optical axis with these two planes. The modified ellipse's foci (empty circles) are located at f'_o = 3500 mm and f'_i = 547.5 mm.

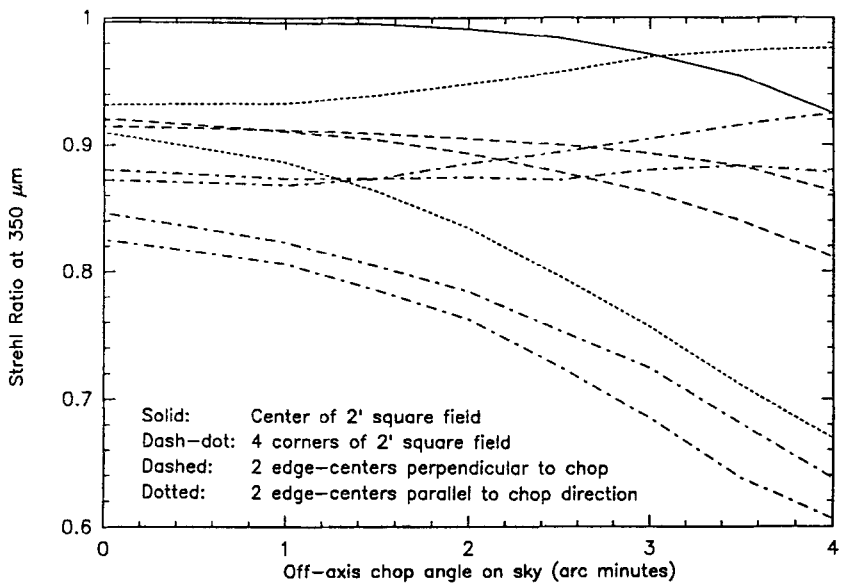

Figure 3: Strehl ratios for the initial ellipsoid, plotted for nine points outlining a 2′ × 2′ square far-field FOV, as a function of the secondary's off-axis chop angle on the sky.

the axis of large cryogenic dewars while also providing sufficient clearance at the sides of the dewar for the input beam. Fig. 1 shows the configuration appropriate to the CSO, which includes two flat mirrors to steer the beam into downward-looking, axisymmetric dewars. The geometry of this initial (hereafter "standard") ellipsoid is defined in Fig. 2, wherein the smaller ellipse plotted depicts a cross-section through the off-axis ellipsoidal mirror's symmetry plane.

The design goal for the relay optics was defined in terms of the Strehl ratio, $S \equiv e^{-(\frac{2\pi\phi_{\rm rms}}{\lambda})^2}$, where $\phi_{\rm rms}$ is the root-mean-square wavefront error in the final aperture plane. At the shortest operating wavelength, 350 μm, the target performance was set at $S \geq 0.9$ across a 2′ square far-field FOV. In addition, this performance needs to be maintained with secondary off-axis chop angles (measured in the far-field) of up to 2′, so that standard "on – off" observing techniques can be used. The standard chop direction, azimuth, is orthogonal to the symmetry plane of the off-axis ellipsoidal mirror.

Fig. 3 plots the resultant Strehl ratios at λ = 350 μm for this standard ellipsoid, calculated with Code V for nine points delimiting the input far-field (the center, corners, and edge-centers of the 2′ square FOV), versus the off-axis angle of the field center provided by chopping the secondary. The curves in Fig. 3 show that S falls well below the target range at the four field corners, and also degrades unacceptably at one of the edge-centers for moderate chop angles (the edge-center furthest from the ellipsoid symmetry plane in the chopped position). This straightforward design thus fails to meet the design goals.

However, there are advantages to a design based on a simple ellipsoidal mirror, including ease of manufacture – large off-axis mirrors can be accurately cut on a numerically-controlled mill simply by tipping an aluminum mirror blank to the appropriate angle and fly-cutting circles in the plane normal to the ellipsoid axis. (Upon polishing to an "optical" finish, surface root-mean-square errors of roughly 3 μm can be achieved). A single focussing mirror also brings a significant optical advantage, in that it provides an image of the aperture stop (the secondary mirror) just prior to the relayed focus (Fig. 1), resulting in a well-concentrated beam between the aperture image and the focal plane. Entry into cryogenic camera dewars of the radiation from relatively large fields is then possible with relatively compact dewar entrance windows, thus minimizing the heat load on the cryogens.

III. MODIFIED ELLIPSOIDS

There are several ways in which a single focusing mirror can be modified to affect its imaging performance (e.g. [10]). First, the ellipsoid of revolution can be generalized to a triaxial figure. Second, the ellipsoidal surface can be modified with higher order corrections, such as higher powers of r^2, where r is the radius normal to the ellipsoid's symmetry axis. Finally, as with a lens, the ellipsoidal mirror's foci can be displaced from the conjugate object and image

planes. All three possibilities were investigated with the aid of Code V.

It is clear that improved imaging can be obtained simply by increasing the focal lengths (and mirror sizes) involved, so an unbiased comparison of these options is possible only by keeping the basic optical configuration fixed. Thus, in the following, the distance, f_o, from the object (Cassegrain focal) plane to the center of the off-axis mirror (see Fig. 2) is held fixed. Also fixed are the reflection angle, θ, that the field-center's chief ray undergoes at the off-axis mirror, and the instrumental focal ratio F_i (and of course the telescope focal ratio F_o). As a result, f_i, the image distance from the mirror (Fig. 2), is also fixed, being given in terms of the other fixed parameters via

$$f_i = f_o \frac{F_i}{F_o}. \tag{1}$$

The focal length, f, of the off-axis mirror, given by the classical formula

$$\frac{1}{f} = \frac{1}{f_o} + \frac{1}{f_i}, \tag{2}$$

is then also fixed.

Of the alternatives listed, the first two fail to improve the imaging substantially, for reasons relatively straightforward to understand. The first possibility, deformation of the ellipsoidal mirror to a triaxial figure, does not yield significant improvement because of the astigmatic nature of the dominant wavefront aberration which applies in the case of off-axis mirror sections located far from the figure symmetry axis. The situation is illustrated in Fig. 4, which shows through-focus geometric spot diagrams for imaging with the standard ellipsoid described above. First, note that in contrast to the case of astigmatism with on-axis optics [11], the aberration pattern here is not symmetric about the central point. It is then necessary to consider only the two orthogonal line foci located just above and below the field center in Fig. 4. As these two field positions call for exactly opposite curvature changes to the mirror surface, it is evident that no single astigmatic surface curvature modification can simultaneously improve the imaging for all field points. Indeed, as can be deduced from more careful study of Fig. 4, the necessary astigmatic surface curvature modification rotates about the mirror normal as the field point rotates about the field center. Indeed, as Fig. 5 illustrates, the dominant effect of introducing unequal curvatures in the mirror's two principal planes is simply to spatially shift the best focus position and the surrounding aberrated focal patterns (both along the optic axis and laterally), without much improvement.

Modifying the surface with higher powers of r^2 is also of limited utility, because maintaining a fixed image location while modifying the surface implies that both the location and slope of the off-axis mirror section's centerpoint (where the chief ray strikes it) must remain unaltered. These two constraints

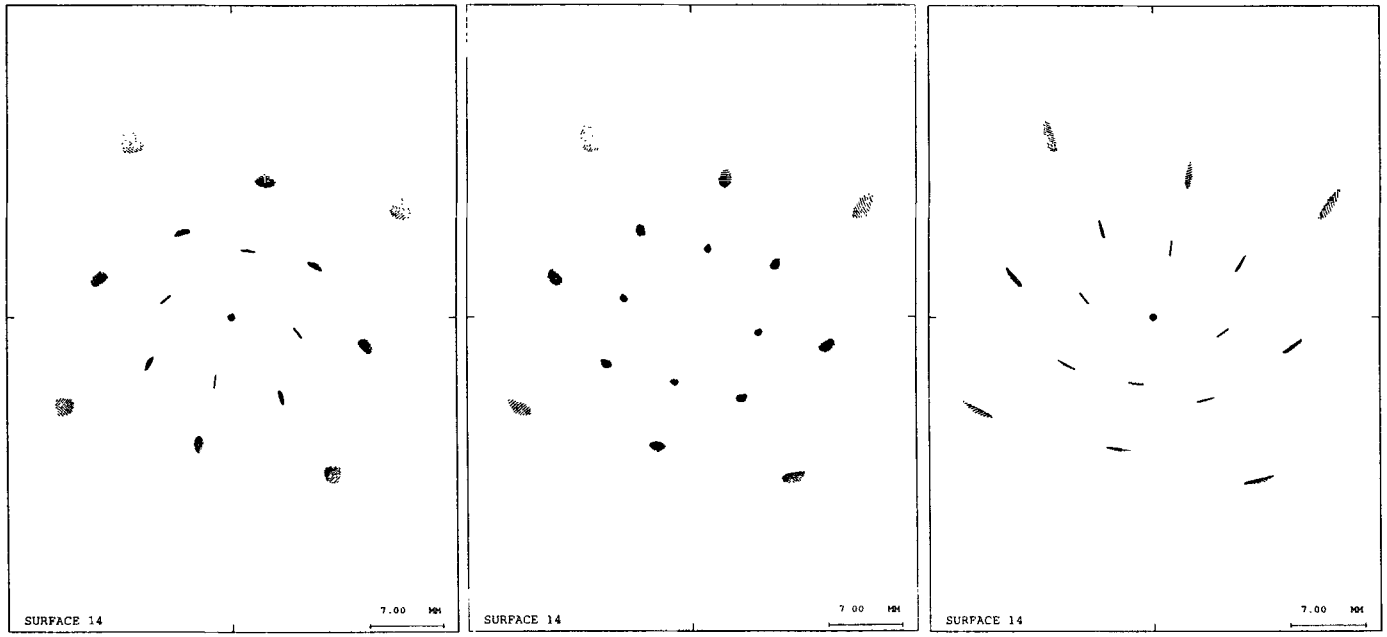

Figure 4: Through-focus ray-trace spot diagrams for the initial ellipsoid of Fig. 2. The center panel shows the calculated intersections of rays with the nominal focal plane, and the left and right panels the spot diagrams 3 mm before and after this plane, respectively. The spot diagrams are for the field center, 8 points outlining the corners and edge-centers of a $1' \times 1'$ object field, and 8 points outlining the corners and edge-centers of a $2' \times 2'$ object field. The spot diagrams are rotated 14° from the vertical because of the departure from the telescope's symmetry plane engendered by mirror M3.

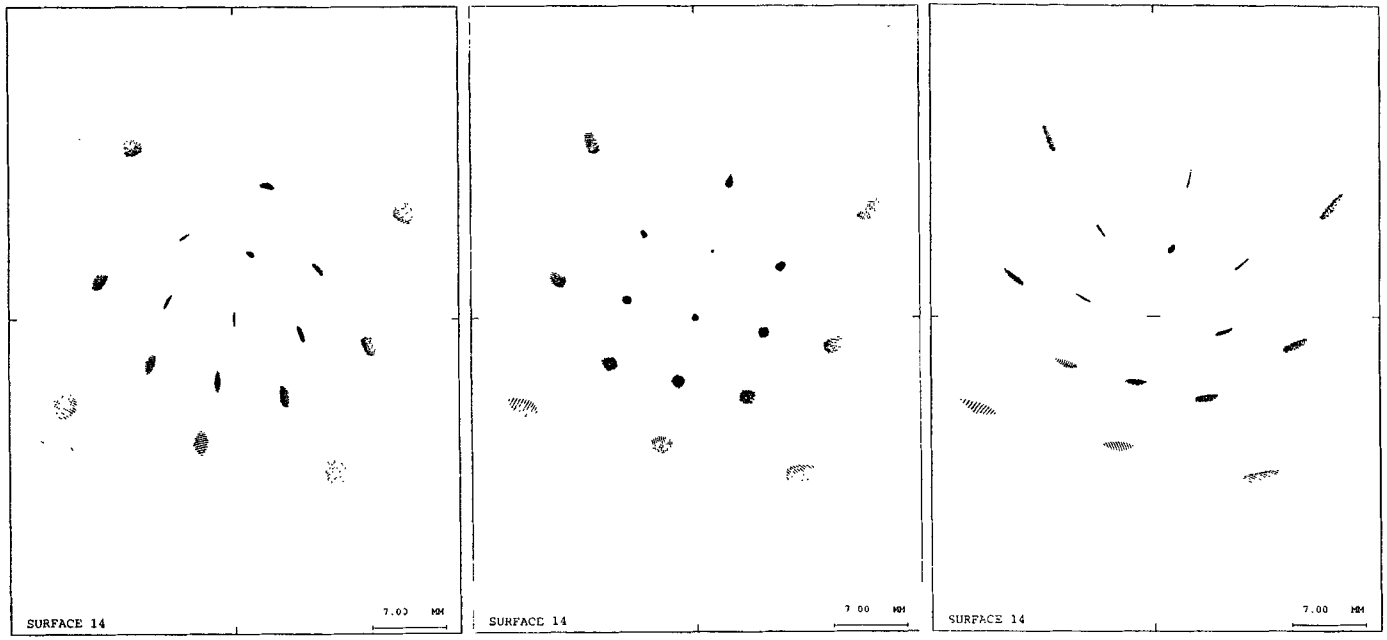

Figure 5: Through-focus spot diagrams with the initial ellipsoid modified slightly – its radius of curvature in the plane orthogonal to the mirror section's symmetry plane (Fig. 2) has been decreased by 5 mm (out of 1284 mm). The spot diagrams shown are for the previous best focal plane (right), as well as 3 mm (center) and 6 mm (left) before this plane. The best focus now lies roughly 3 mm ahead of the previous best focal plane, and occurs for an object location roughly $1'$ above the field center.

thus allow little freedom until at least three terms (up to r^8) are included in the expansion, at which point a ripply mirror is in hand. In addition, since these higher order terms are azimuthally symmetric about the mirror axis, they bear some resemblance to the astigmatic surface deformations discussed above, and, for like reasons, cannot compensate for astigmatic errors which vary with field position. Of course the possibility of improved imaging using one or both of these techniques in concert with multiple focusing elements remains (e.g. [12]).

On the other hand, significant improvement results from a shift to a different ellipsoid. In particular, just as with a lens, the basic ellipsoidal mirror can be modified so that its geometric foci are displaced along the input and output optical axes, while keeping the conjugate object and image planes, and the beam focal ratios fixed. The relevant geometry is depicted in Fig. 2, in which cross-sections through both the original and modified ellipsoids are shown. For fixed conjugate planes at f_o and f_i from the mirror surface, as the ellipsoid's input-side geometric focus is translated along the telescope/optical axis toward the secondary mirror, i.e., away from the off-axis mirror section (thus moving it from f_o to f_o'), the ellipsoid's second focus moves inward from the image plane, toward the ellipsoidal mirror (from f_i to f_i'), while satisfying

$$\frac{1}{f_i'} + \frac{1}{f_o'} = \frac{1}{f} \tag{3}$$

As can be seen in Fig. 2, this modification results in two beneficial changes: the modified ellipsoid is larger than the original, and the desired mirror section is closer to the modified ellipsoid's symmetry axis. As the desired mirror section is then less off-axis, the imaging across the field is in general improved (but imaging at the field center degrades slightly). However, one detrimental change also results from these alterations: the modified ellipsoid's major axis now intersects the Cassegrain focal plane off the field center.

It is straightforward to relate the parameters of the family of modified ellipsoids to those of the original ellipsoid. The modified eccentricity, $\epsilon' = c'/a'$, is determined by the ellipsoid's major axis length, $2a'$, given as usual by

$$2a' = f_o' + f_i', \tag{4}$$

and the axial inter-focal distance, $2c'$, given by

$$2c' = \sqrt{f_o'^2 + f_i'^2 - 2f_o'f_i'\cos\theta}. \tag{5}$$

By dropping a perpendicular from f_i' to the incoming chief ray, it can also be seen that α, the angle between the ellipsoid and telescope axes is given by

$$\sin\alpha = \frac{f_i'}{2c'}\sin\theta. \tag{6}$$

Of course these equations hold also for the original ellipsoid by removing the primes. The final parameter of interest is the modified ellipsoid's vertex radius of curvature, $\rho'_v = a'(1 - \epsilon'^2) = (a'^2 - c'^2)/a'$, which by substituting for a' and c' from equations (4) and (5), and then using (2) and (3), yields

$$\rho'_v = \frac{(1+\cos\theta)}{\frac{1}{f'_i} + \frac{1}{f'_o}} = \frac{(1+\cos\theta)}{\frac{1}{f_i} + \frac{1}{f_o}}. \tag{7}$$

Because f_o, f_i, and θ are fixed by design, ρ'_v is invariant. Thus all of the modified ellipsoid's parameters can be derived easily from f'_o and the fixed initial parameters. In particular, it is easy to show that α decreases asymptotically to zero as f'_o increases without bound, and that ϵ' increases monotonically to unity, yielding the limiting paraboloid.

However, due to the interplay of the various geometric modifications discussed above, it is not desirable to go to the parabolic limit. Rather, as made clear by numerical calculations with Code V, the performance peaks for ellipsoids with $f'_o \approx 2f_o$. The improved Strehl ratios for this case, plotted in Fig. 6, show that now $S > 0.88$ over the entire $2' \times 2'$ FOV, falling slightly below the goal of 0.9 in only one small corner of the field. S also shows little degradation with chopper angle for throws of up to $2'$ off axis. As the residual aberrations are rather small, the achieved performance should meet the needs of foreseen submillimeter array instruments for some time to come.

IV. RELATED CAMERA OPTICS

As with lens-based designs, subsequent camera optics can be enlisted to further improve imaging performance. One of the first instruments to use these relay optics is the CSO's Submillimeter High Angular Resolution Camera (SHARC), and its design incorporates an additional ellipsoid (which reimages a cryogenic field stop onto the detector array), to partially cancel the comatic aberration contribution [1,8]. Fig. 7, which shows SHARC's resultant Strehl ratios across the same $2' \times 2'$ design FOV (from [1]), indicates that S exceeds 0.95 across the entire field, even with secondary chop angles of up to $2'$. Comparing Figs. 3, 6 & 7, which are all on the same scale, makes clear that a pair of properly designed off-axis ellipsoidal mirrors can keep aberrations to negligible levels across sizable FOVs, even allowing for relatively large reflection angles at the focusing mirrors, and large secondary chop angles.

V. DUAL FOCI

Finally, the desire for two equivalent instrument foci was met by installing the flat mirror M3 (Fig. 1) on a turntable, which is used to direct the telescope beam to either side of the telescope's symmetry plane (the plane bisecting the telescope's elevation axis). Identical versions of mirrors M4 (Fig. 1) then steer the two beams into parallel vertical planes symmetrically placed 11 inches

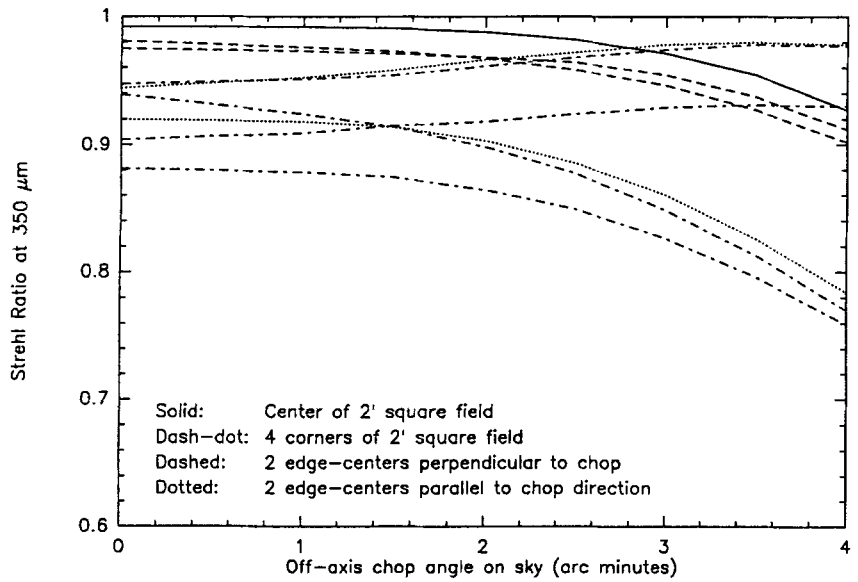

Figure 6: Strehl ratios vs. off-axis chop angle for the modified ellipsoid. The nine curves delineate the boundary of the same 2′ × 2′ field as in Fig. 3.

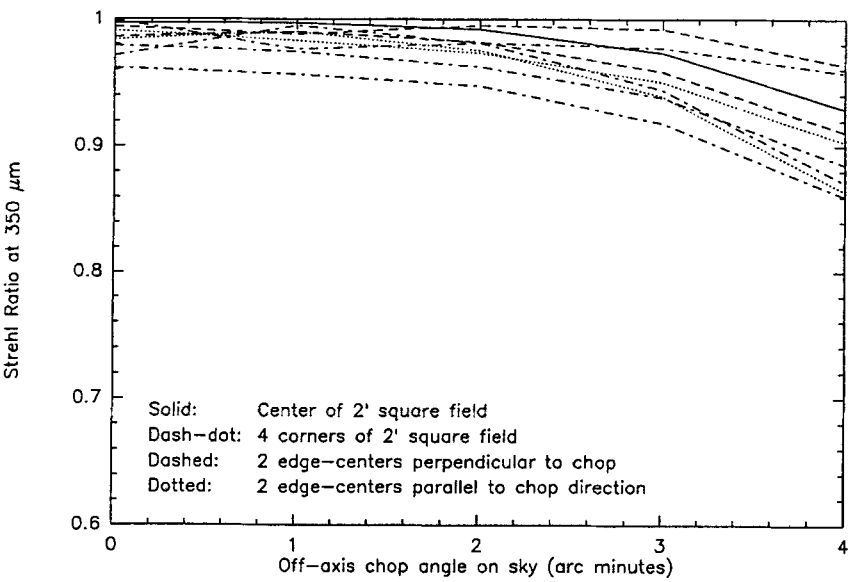

Figure 7: Strehl ratios vs. off-axis chop angle for SHARC (from ref [1]). The nine curves delineate the boundaries of the same 2′ × 2′ field as in Fig. 3.

to either side of the telescope symmetry plane, after which a pair of identical ellipsoids (M5 in Fig. 1) provide the focusing in each of the optical trains. Fixed stops on M3's turntable allow rapid and reproducible switching between the two optical trains, while the "optical" polish of the numerically-milled ellipsoidal mirrors allows for rapid optical alignment of both optical trains with a HeNe laser. Prospective users of the relay optics can find a complete description of the dual system's three-dimensional configuration, as well as of the instrument mounting interfaces, in CSO Optics Memo #4, available upon request.

ACKNOWLEDGEMENTS

I wish to heartily thank Walt Schaal for his efforts in designing the relay optics mechanical support structure, M. A. Gerfen for his careful machining of the off-axis mirrors, T. R. Hunter and J. H. Lacy for helpful comments on the manuscript, and many parties interested in using the relay optics for informative discussions. This work was supported by NSF grant AST-9313929.

REFERENCES

[1] T.R. Hunter, D.J. Benford & E. Serabyn 1996, Pub. Ast. Soc. Pac., in press.

[2] N. Wang, T.R. Hunter, D.J. Benford, E. Serabyn, D.C. Lis *et al.* 1996, Appl. Opt., in press.

[3] D.A. Schleuning, C.D. Dowell, R.H. Hildebrand, & S.R. Platt, 1996, preprint.

[4] W.S. Holland, P.A.R. Ade, M.J. Griffin, I.D. Hepburn, D.G. Vickers *et al.* 1996, Int'l. J. Infrared & Millimeter Waves 17, 669.

[5] I. S. McLean 1994, *Infrared Astronomy with Arrays: The Next Generation* (Kluwer: Dordrecht).

[6] S.H. Moseley, J.C. Mather, & D.J. McCammon 1984, J. Appl. Phys. 56, 1257.

[7] R. Padman 1995, in *Multi-Feed Systems for Radio Telescopes*, ASP Conf. Ser. Vol. 75, ed. D.T. Emerson & J.M. Payne, p. 3.

[8] E. Serabyn 1995, in *Multi-Feed Systems for Radio Telescopes*, ASP Conf. Ser. Vol. 75, ed. D.T. Emerson & J.M. Payne, p. 74.

[9] E.V. Loewenstein, D.R. Smith, & R.L. Morgan 1973, Appl. Opt. 12, 398.

[10] Code V Reference Manual, Optical Research Associates, 550 North Rosemead Blvd., Pasadena CA 91107.

[11] W.T. Welford 1986, *Aberrations of Optical Systems* (Adam Hilger: Bristol).

[12] W.K. Gear & C.R. Cunningham 1995, in *Multi-Feed Systems for Radio Telescopes*, ASP Conf. Ser. Vol. 75, ed. D.T. Emerson & J.M. Payne, p. 215.